(p,xn) and (p,pxn) Reactions of Yttrium-89 with 5–85-MeV Protons*†

G. B. SAHA AND N. T. PORILE
Radiochemistry Laboratory, Department of Chemistry, McGill University, Montreal, Canada,
and
Department of Chemistry, Purdue University, Lafayette, Indiana

AND

L. YAFFE
Radiochemistry Laboratory, Department of Chemistry, McGill University, Montreal, Canada

(Received 21 October 1965)

Excitation functions for the (p,xn) ($x=1$–4) and (p,pxn) ($x=1$–5) reactions of Y^{89} with 5–85 MeV protons have been determined. Isomer ratios have been measured for the $(p,p2n)$, $(p,p3n)$, and $(p,p4n)$ reactions. The cross sections have been compared with the results of a cascade-evaporation calculation based on the recent code by Chen *et al.* This calculation predicts close to 100% compound-nucleus formation up to bombarding energies of about 35 MeV, and the excellent agreement with experiment attests to the validity of this prediction. A number of discrepancies between experiment and calculation are noted at higher energies. These are due to the fact that the calculation by Chen *et al.* appears to overestimate the amount of compound-nucleus formation in the energy range of 45–85 MeV.

I. INTRODUCTION

THE study of nuclear reactions in the energy range of approximately 10–100 MeV is of considerable interest in view of the change in reaction mechanism occurring in this region. At the lower end of this interval most reactions involve the formation and subsequent decay of a compound nucleus. At the upper end, direct processes predominate and the reactions have been described in terms of a two-step cascade-evaporation process. Considerable insight has been gained in recent years through the comparison of experimental data with the results of Monte Carlo cascade-evaporation calculations. At low energies the computations are based on the statistical theory of nuclear reactions. The calculation by Dostrovsky *et al.*[1] has been used in this way to calculate excitation functions for a variety of reactions. At higher energies the cascade process becomes of importance. A number of Monte Carlo treatments of this process, based on differing nuclear models and approximations, have been performed.[2–4] Most recently, Chen *et al.*[4] performed a rather sophisticated calculation of this type using a non-uniform nucleon density distribution and considering reflection and refraction of the cascade particles at the surfaces of changing potential. The combination of cascade and evaporation calculations yields cross sections which may then be compared with experiment as an overall test of this model.

The number of experimental studies below 100 MeV that have been compared with this theory is very limited. Porile *et al.*[5] measured excitation functions for the reactions of Ga^{69} and Ga^{71} with 15–56 MeV protons. These authors compared their results at 46 MeV with cascade-evaporation calculations based on the treatments by Metropolis *et al.*[2] and Dostrovsky *et al.*[1] Proton induced reactions in the energy range of interest have also been reported for a few additional medium-weight target elements[6–8] although no comparisons with calculations were given. The present investigation involves the measurement of excitation functions for the (p,xn) and (p,pxn) reactions of Y^{89} with 5–85 MeV protons. The results are then used to test the cascade-evaporation model as based on the codes by Chen *et al.*[4] and Dostrovsky *et al.*[1] On the basis of these comparisons it is then possible to draw some conclusions concerning the relative importance of compound-nuclear and direct processes throughout the energy range of interest.

II. EXPERIMENTAL

The target material was a mixture of spectroscopically pure Y_2O_3 and CuO powders. The CuO was used to monitor the intensity of the proton beam by means of the $Cu^{65}(p,pn)$ or $Cu^{63}(p,n)$ reactions. A known amount of the mixture was loaded into an aluminum tube which was then flattened in order to minimize the energy degradation of the beam and mounted on the cyclotron probe. Irradiations were carried out in the internal proton beam of the McGill synchrocyclotron at a radius corresponding to the desired energy. Irradiations were made in the energy range of 5–85 MeV at 3-MeV inter-

* Supported by a grant from the National Research Council, Canada, and in part by the U. S. Atomic Energy Commission.

† Based on a dissertation submitted by G. B. Saha in partial fulfillment of the requirements for the Ph.D. degree at McGill University, Montreal, Quebec, Canada.

[1] I. Dostrovsky, Z. Fraenkel, and G. Friedlander, Phys. Rev. **116**, 683 (1959).

[2] N. Metropolis, R. Bivins, M. Storm, A. Turkevich, J. M. Miller, and G. Friedlander, Phys. Rev. **110**, 185 (1958).

[3] H. W. Bertini, Phys. Rev. **131**, 1801 (1963).

[4] C. Chen, Z. Fraenkel, G. Friedlander, J. R. Grover, J. M. Miller, and Y. Shimamoto (to be published).

[5] N. T. Porile, S. Tanaka, H. Amano, M. Furukawa, S. Iwata, and M. Yagi, Nucl. Phys. **43**, 500 (1963).

[6] J. W. Meadows, Phys. Rev. **91**, 885 (1953).

[7] R. A. Sharp, R. M. Diamond, and G. Wilkinson, Phys. Rev. **101**, 1493 (1956).

[8] S. Hontzeas and L. Yaffe, Can. J. Chem. **41**, 2194 (1963).

vals up to 48 MeV, and then at 6-MeV intervals up to 85 MeV. Duration of irradiation varied from 15 to 70 min and the beam intensity ranged from 0.5 to 1 μA.

After irradiation the target was dissolved in concentrated HCl+H_2O_2 and zirconium, yttrium, and either copper or zinc were chemically separated. Zirconium and yttrium were first separated from copper or zinc by elution with 6N HCl from a Dowex-1 ion-exchange column. The separation of zirconium involved the successive precipitation of $ZrO(H_2PO_4)_2$, $BaZrF_6$, $BaSO_4$, and $Zr(OH)_4$. This cycle was repeated and the final precipitate dissolved in 4N HCl for the activity measurements. Chemical yields were determined by spectrophotometry using the "Thoron" complexing reagent.

After removal of zirconium from the target solution, yttrium was separated by means of several cycles of YF_3 and $Y(OH)_3$ precipitations. Yttrium was then extracted from concentrated HNO_3 solution into tributyl phosphate, back-extracted with water, precipitated with NH_4OH and dissolved in 4N HCl for the activity measurements. Chemical yields were determined spectrophotometrically using sodium alizarine sulphonate as the complexing reagent.

Following elution of zirconium and yttrium, copper and zinc were separated by elution with 2N HCl and H_2O, respectively. The chemical yields of these elements were determined by titration with ethylenediamine tetra-acetic acid (EDTA).

After chemical separation, known aliquots of the samples were transferred to glass vials for the activity measurements. A calibrated 3-in.×3-in. NaI(Tl) scintillation detector, coupled to a 100-channel pulse-height analyzer, was used to detect the characteristic gamma rays of particular nuclides. The disintegration rate of nuclides decaying by positron emission was determined with a 511 keV-511 keV gamma-ray coincidence spectrometer. Two $1\frac{1}{2}$-in.×1-in. NaI(Tl) detectors were placed at 180° with respect to the source. In order to correct for the rare chance of accidental coincidences, one of these detectors was paired with a third $1\frac{1}{2}$-in. ×1-in. NaI(Tl) crystal placed at 90° with respect to it. All three detectors subtended the same solid angle relative to the source. The coincidence unit was calibrated with a standard Na^{22} source and its efficiency was about 0.1%. The pertinent decay-scheme information[9] as well as the detection methods used for the various nuclides of interest are summarized in Table I.

The counting data were resolved into individual components either graphically or with the CLSQ computer program.[10] Counting rates at end of bombardment were converted to disintegration rates by applying corrections for chemical yields, aliquots, counter efficiencies, branching ratios, and internal conversion coefficients. Wherever appropriate, corrections were applied for the formation of a particular yttrium nuclide

TABLE I. Decay-scheme data and detection methods for the observed radioactive nuclides.

Nuclide	Reaction	Half-life	Radiation followed	Branch abundance	Detection technique
Zr^{89}	(p,n)	78.6 h	β^+	22%	CC[a]
			0.908 MeV γ	100%	PHA[a]
Zr^{88}	($p,2n$)	85 day	0.39 MeV γ	100%	PHA
Zr^{87}	($p,3n$)	100 min	β^+	83%	CC
Zr^{86}	($p,4n$)	17 h	0.241 MeV γ	100%	PHA
Y^{88}	(p,pn)	105 day	0.90 MeV γ	94%	PHA
			1.84 MeV γ	100%	
Y^{87m}	($p,p2n$)	13.2 h	0.381 MeV γ	100%	PHA
Y^{87g}	($p,p2n$)	80 h	0.48 MeV γ	97.7%	PHA
Y^{86m}	($p,p3n$)	48.5 min	0.208 MeV γ	100%	PHA
Y^{86g}	($p,p3n$)	14.7 h	β^+	30%	CC
Y^{85m}	($p,p4n$)	2.68 h	β^+	55%	CC
Y^{85g}	($p,p4n$)	5 h	β^+	70%	CC
Y^{84}	($p,p5n$)	40 min	β^+	86.5%	CC
Cu^{64}	(p,pn)	12.7 h	β^+	19%	CC
					PHA
Zn^{63}	(p,n)	38.3 min	β^+	93%	CC
					PHA

[a] PHA—100-channel pulse-height analyzer; CC—(0.511-MeV gamma)–(0.511-MeV gamma) coincidence counter.

TABLE II. Assumed values of the monitor reaction cross sections.

Energy (MeV)	$Cu^{63}(p,n)Zn^{63}$ cross section[a] (mb)	$Cu^{65}(p,pn)Cu^{64}$ cross section[b] (mb)
5	43	...
8.5	359	...
12	513	...
15	470	...
18.5		124
21.5		340
24.8		486
27		476
27.5		456
30.5		378
33.5		328
36.8		290
40		264
42		252
45		235
48		220
54		198
57		188
60		180
66		167
72		156
78		148
85		140

[a] Taken from Ghoshal, Ref. 11.
[b] Taken from Meghir and Yaffe, Ref. 12.

[9] *Nuclear Data Sheets*, compiled by K. Way *et al.* (Printing and Publishing Office, National Academy of Sciences—National Research Council, Washington, D. C.), NRC-60-3-56, 60-3-63, 60-3-64, 59-3-13. Aslo D. M. Van Patter and S. M. Shafroth, Nucl. Phys. **50**, 115 (1964); J. I. Rhode, O. E. Johnson, and W. G. Smith, Phys. Rev. **129**, 815 (1963); T. Yamazaki, H. Ikegami, and M. Sakai, Nucl. Phys. **30**, 68 (1962); Y. E. Kim, D. J. Horen, and J. M. Hollander, *ibid.* **31**, 447 (1962); I. Dostrovsky, S. Katcoff, and R. W. Stoenner, Phys. Rev. **132**, 2600 (1963); V. Maxia, W. H. Kelley, and D. J. Horen, J. Inorg. Nucl. Chem. **24**, 1175 (1962).

[10] J. B. Cumming, Natl. Acad. Sci.—Natl. Res. Council, Nucl. Sci. Series, NAS-NS-3107, 1962, p. 25.

through decay of its zirconium precursor both during irradiation and prior to the separation time.

The beam intensity was monitored by means of the $Cu^{63}(p,n)$ reaction up to 15 MeV and the $Cu^{65}(p,pn)$ reaction at higher energies. The cross sections for these reactions were taken from Ghoshal[11] and Meghir and Yaffe,[12] respectively, and they are summarized in Table II.

III. RESULTS

The measured cross sections of the (p,xn) reactions are tabulated in Table III and those of the (p,pxn) reactions in Table IV. Cross sections for the formation of isomeric states in the $(p,p2n)$, $(p,p3n)$, and $(p,p4n)$ reactions as well as the corresponding isomer ratios are presented in Tables V–VII. Plots of the excitation functions for the (p,xn) and $p,pxn)$ reactions are given in Figs. 1 and 2, respectively.

The quoted uncertainties include both the random errors associated with the determination of photopeak areas, decay curve analysis, chemical yields, etc., as well as the systematic errors associated with the counter efficiencies and spread in beam energy. The additional errors due to the uncertainties in the cross sections of the monitor reactions and in the assumed decay schemes have not been included. The random error, as determined from the scatter of the points on the excitation functions, is considerably smaller than the estimated total error of 11–22%.

TABLE III. Experimental cross sections of (p,xn) reactions.

Bombarding energy (MeV)	$\sigma(p,n)$ (mb)	$\sigma(p,2n)$ (mb)	$\sigma(p,3n)$ (mb)	$\sigma(p,4n)$ (mb)
5	50 ± 5.5			
8.5	352 ±39			
12	720 ±79			
15	712 ±78	68 ± 8.8		
18.5	552 ±61	352 ± 46		
21.5	395 ±43	495 ± 64		
24.8	194 ±21	1252 ±163		
27	...	1248 ±162		
27.5	103 ±11	1318 ±171		
30.5	61.4± 6.8	{828 ±108 896 ±116	55 ± 6.6	
33.5	43 ± 4.7	506 ± 66	118 ±14	
36.8	45 ± 5	329 ± 43	313 ±38	
40	...	...	385 ±46	
42	37 ± 4.1	172 ± 22	{333 ±40 349 ±42	
45	...	...	299 ±36	26.6± 4.3
48	29.4± 3.2	112 ± 15	168 ±20	57 ± 9.1
54	29.7± 3.3	82.5± 11	91 ±11	78 ±12.5
57	...	...	...	81.5±13
60	23.3± 2.6	73.4± 9.5	55.4± 6.6	63 ±10
66	19.7± 2.2	60 ± 7.8	54 ± 6.5	42 ± 6.7
72	17 ± 1.9	54 ± 7	47.5± 5.7	32 ± 5.1
78	14.4± 1.6	46 ± 6	36.5± 4.4	27.7± 4.4
85	12 ± 1.3	41 ± 5.3	31.5± 3.8	22 ± 3.5

[11] S. N. Ghoshal, Phys. Rev. **80**, 939 (1950).
[12] S. Meghir and L. Yaffe (to be published).

TABLE IV. Experimental cross sections of (p,pxn) reactions.

Bombarding energy (MeV)	$\sigma(p,pn)$ (mb)	$\sigma(p,p2n)$[a] (mb)	$\sigma(p,p3n)$[a] (mb)	$\sigma(p,p4n)$[a] (mb)	$\sigma(p,p5n)$ (mb)
15	3.6± 0.5				
18.5	38 ± 5				
21.5	141 ±18				
24.8	257 ±33	1.4			
27	...	3.5			
27.5	304 ±40	...			
30.5	365 ±47	95.7			
33.5	310 ±40	229			
36.8	283 ±37	284	10.7		
40	...	320	...		
42	231 ±30	{370 352	19.5		
45	...	395	61.5		
48	228 ±30	340	126.5		
54	186 ±24	263	208		
57	...	...	209		
60	199 ±26	218	237	57.6	
66	177 ±23	164	161	{134.5 155	0.37 ±0.074
72	175 ±23	158.6	121	{163 141.4	...
78	162 ±21	155.6	117.5	{136.5 133	11 ±2.2
85	144 ±19	128.5	105.6	{109 127	24 ±4.8

[a] Errors for the cross sections of individual isomers are given in Tables V, VI, VII.

TABLE V. Experimental cross sections and isomeric ratios of Y^{87m} $(\frac{9}{2}+)$ and Y^{87g} $(\frac{1}{2}-)$.

Bombarding energy (MeV)	σ_H (mb)[a]	σ_L (mb)[a]	σ_H/σ_L[a]
24.8	0.40± 0.08	1.0± 0.2	0.4 ±0.08
27	1.8 ± 0.36	1.7± 0.34	1.06±0.22
30.5	64 ±13	31.7± 6.3	2.02±0.42
33.5	159 ±32	70 ±14	2.27±0.48
36.8	201 ±40	83 ±17	2.42±0.51
40	230 ±46	90 ±18	2.56±0.54
42	{281 ±56 251 ±50	{ 89.2±18 101 ±20	{3.15±0.66 2.5 ±0.53
45	282 ±56	113 ±23	2.5 ±0.53
48	245 ±49	95 ±19	2.6 ±0.55
54	180 ±36	83 ±17	2.17±0.46
60	146 ±29	72 ±14	2.03±0.43
66	111 ±22	53 ±11	2.09±0.44
72	111 ±22	47.6± 9.5	2.33±0.49
78	107 ±21	48.6± 9.7	2.20±0.46
85	88 ±18	40.5± 8.1	2.17±0.46

[a] Subscript H refers to the high-spin isomer and L to the low-spin isomer.

TABLE VI. Experimental cross sections and isomeric ratios of Y^{86m} (8+) and Y^{86g} (4−).

Bombarding energy (MeV)	σ_H (mb)	σ_L (mb)	σ_H/σ_L
45	17.5± 4.4	44 ±11	0.40±0.11
48	56.5±14	70 ±18	0.81±0.23
54	115 ±29	93 ±23	1.24±0.35
57	106 ±27	103 ±26	1.03±0.29
60	135 ±34	102 ±26	1.32±0.37
66	87 ±22	74 ±19	1.18±0.33
72	64 ±16	57.5±14	1.11±0.31
78	64.5±16	53 ±13	1.22±0.34
85	55.2±14	50.4±13	1.10±0.31

TABLE VII. Experimental cross sections and isomeric ratios of Y^{85m} ($\frac{1}{2}-$) and Y^{85g} ($\frac{9}{2}+$).

Bombarding energy (MeV)	σ_L (mb)	σ_H (mb)	σ_H/σ_L
60	4.6±0.55	53± 6.4	11.50±1.03
66	32.5±3.9	102±12	3.14±0.28
	57 ±6.8	98±12	1.72±0.15
72	58 ±7	105±12	1.81±0.16
	52.4±6.3	89±11	1.70±0.15
78	46.5± 5.6	90±11	1.94±0.17
	44 ±5.3	89±11	2.02±0.18
85	43 ±5.2	66± 8	1.53±0.14
	40 ±4.8	87±11	2.18±0.20

The results of this study may be compared with some previous measurements of proton-induced reactions in Y^{89}. Caretto and Wiig[13] determined the cross-sections for a number of reactions in the energy interval of 60–240 MeV. Their results at 60 MeV for the (p,n), ($p,2n$), and (p,pn) are larger than our values by about a factor of two. On the other hand, the cross sections for the ($p,4n$) and ($p,p2n$) reactions agree with the present data within the experimental uncertainties.

The excitation function for the $Y^{89}(p,pn)$ reaction has recently been determined by Gusakow.[14] His results are in very good agreement with the present values above 48 MeV. However, at lower energies his cross sections are lower than the present values by a factor of 1.5–2.0.

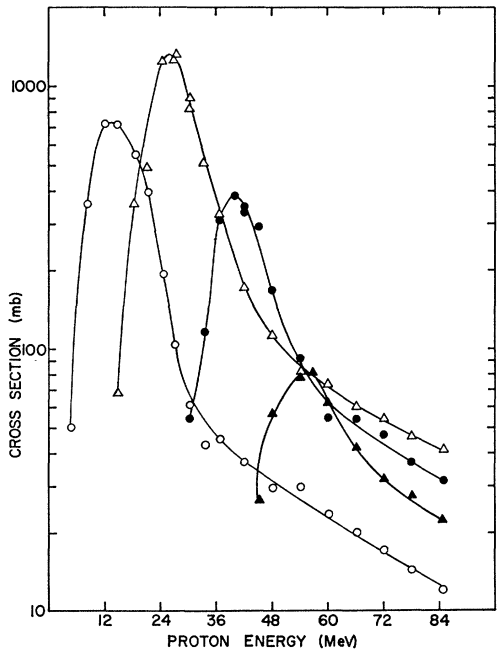

FIG. 1. Excitation functions for the $Y^{89}(p,xn)$ reactions; ○—(p,n); △—($p,2n$); •—($p,3n$); ▲—($p,4n$).

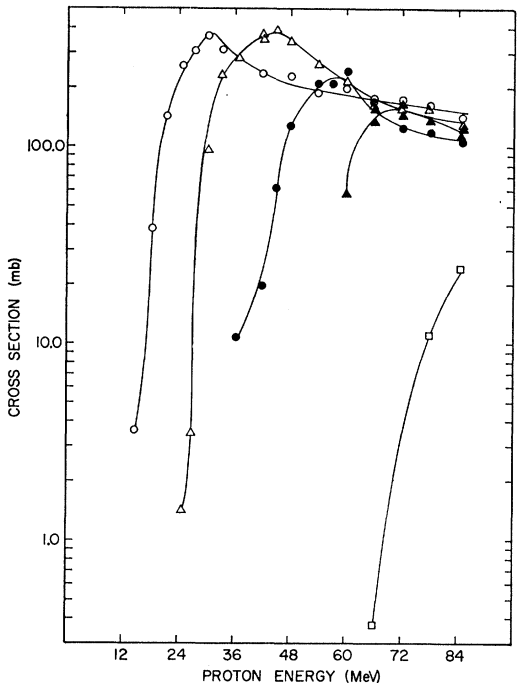

FIG. 2. Excitation functions for the $Y^{89}(p,pxn)$ reactions; ○—(p,pn); △—($p,p2n$); •—($p,p3n$); ▲—($p,p4n$); □—($p,p5n$).

This discrepancy may be due to possible differences in the energy spread of the proton beams in the two accelerators. At low energies the excitation functions for the $Y^{89}(p,pn)$ and the monitor reactions have a strong energy dependence and so are sensitive to small differences in proton energy.

The cross sections of the (p,n), ($p,2n$) and (p,pn) reactions of Y^{89} have recently been determined by Chen-peng *et al.*[15] in the energy range of 120–670 MeV. Their values at 120 MeV are 5.8 mb, 15.0 mb, and 95.5 mb, respectively. These results are in line with the trend observed in the present work.

IV. DISCUSSION

A. Qualitative Considerations

In this sub-section we shall examine various features of the results in a qualitative way. A comparison with the results of statistical theory and cascade-evaporation calculations is presented in the following sub-section.

The excitation functions for the (p,xn) reactions, Fig. 1, exhibit the following features of interest. The cross section of a given reaction increases sharply with energy above the reaction threshold and then, as further neutron emission becomes energetically possible, begins to decrease. This decrease is very marked for the first 20–25 MeV past the peak but becomes much less pro-

[13] A. A. Caretto and E. O. Wiig, Phys. Rev. **115**, 1238 (1959).
[14] Mark Gusakow, Ph.D. thesis, Faculté des Sciences de l'Université de Paris, 1962 (unpublished).
[15] W. Chen-peng, I. Levenberg, V. Pokrovsky, L. Tarasova, and I. Yutlandov, Joint Institute for Nuclear Research, Dubna, P-2218, 1965 (unpublished).

nounced at higher energies. These high-energy tails of the excitation functions are a well-known manifestation of the cascade process. Similar results have been previously found in a number of other studies in the mass and energy range of present interest.[5–8]

The (p,pxn) reactions have excitation functions that differ in one striking respect from those of the (p,xn) reactions. As seen in Fig. 2, the cross sections decrease only slightly above the peak and their magnitude generally remains above 100 mb at the highest energy. This difference between the (p,xn) and (p,pxn) reactions is also illustrated in Fig. 3, which shows the ratios of cross sections of isobaric nuclides formed as a result of (p,xn) and $[p, p(x-1)n]$ reactions. It is seen that, except near the reaction thresholds, the isobaric ratios decrease steadily with increasing bombarding energy and begin to level off at values of 0.2–0.3 at the highest energy. This trend can be attributed to the increasing importance of proton emission with increasing bombarding energy. Presumably, the principal mechanism for proton emission at the higher energies is inelastic scattering in the diffuse surface of the nucleus.

The same trends are also evident from an examination of the probability for the occurrence of reactions in which no charged particles are emitted compared with that for reactions in which a singly charged particle plus a number of neutrons are emitted. These quantities, denoted by f_n and f_p, respectively, are given by the ratio of the sum of the (p,xn) or (p,pxn) cross sections to the total reaction cross section as calculated in the manner of Dostrovsky *et al.*[1] The dependence of f_n and f_p on bombarding energy is shown in Fig. 4. As it was impossible to measure the cross sections of all (p,xn) and (p,pxn) reactions that occurred in the energy range of interest, the values of f_n and f_p had to be corrected. The cross sections for the unmeasured (p,p'), $(p,5n)$, and $(p,6n)$ reactions were estimated on the basis of the cascade-evaporation calculation and their effect is indicated by the arrows on the curves. The strikingly different shape of the f_n and f_p curves can be readily explained in terms of the assumed reaction mechanism. At low energies the compound-nucleus-formation cross section approaches the total reaction cross section and neutron evaporation is therefore more probable than proton emission. As the bombarding energy increases, proton emission becomes increasingly important both as a result of the increasing probability for evaporation from a compound nucleus and that of reemission in a direct process. The large and nearly constant value of f_p above 50 MeV is suggestive of a process consisting of a (p,p') cascade followed by neutron evaporation. It is of interest to note that the sum of f_n and f_p is approximately unity up to a bombarding energy of 40 MeV. Above this energy reactions involving the net loss of more than one charge unit become of importance and account for about 60% of the reaction cross section at 85 MeV.

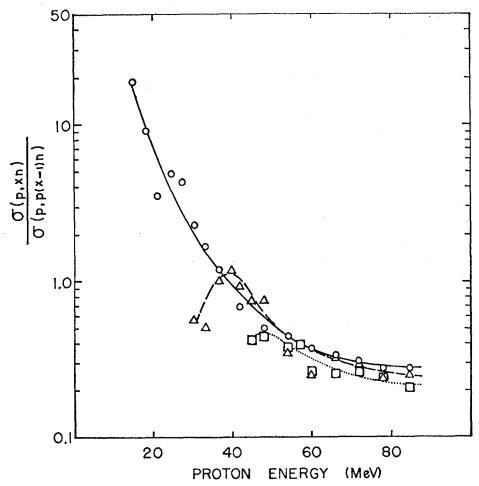

FIG. 3. Energy dependence of isobaric cross-section ratios. ○—$\sigma(p,2n)/\sigma(p,pn)$ (solid curve); △—$\sigma(p,3n)/\sigma(p,p2n)$ (dashed curve). □—$\sigma(p,4n)/\sigma(p,p3n)$ (dotted curve).

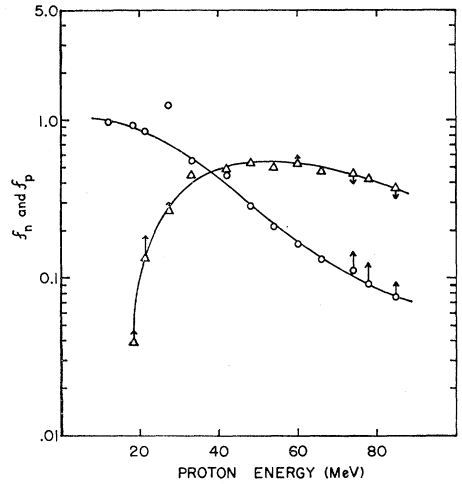

FIG. 4. Variation of f_n and f_p with incident proton energy. ○—f_n (fraction of total reaction cross section involving only neutron emission); △—f_p (fraction of total reaction cross section involving loss of one charge unit). The arrows represent correction for unmeasured reactions.

Another interesting feature of the excitation functions is the variation of the peak energies and cross sections with the number of emitted neutrons, summarized in Table VIII. It is seen that for reactions involving the emission of more than two neutrons, the peak cross sections decrease as the number of emitted neutrons increases. This trend results from the proliferation of competing reactions coupled with a nearly constant value of the total reaction cross section at the higher energies. It can be expected that this trend should be most important in the case of reactions which proceed largely by compound nucleus formation at the peak energies. Direct reactions are less susceptible to competing decay modes because the emitted knock-on nucleons usually have much higher energies than

TABLE VIII. Peak cross sections and peak energies of various reactions.

Reaction	Peak energy (MeV)	Peak cross section (mb)
(p,n)	13	720
(p,2n)	26	1380
(p,3n)	40	380
(p,4n)	55	80
(p,pn)	30	350
(p,p2n)	46	370
(p,p3n)	59	218
(p,p4n)	70	165

evaporated particles. The (p,xn) reactions do indeed display a much sharper decrease in peak cross sections than the (p,pxn) reactions in line with this expectation.

The peak energies of the excitation functions show a systematic increase with the number of emitted neutrons. This behavior is, of course, primarily due to the increase in the reaction thresholds. In addition to this factor, the kinetic energy associated with the emitted nucleons and photons also increases with the number of emitted neutrons. This is shown in Figs. 5 and 6 which are plots of the excitation functions for the (p,xn) and (p,pxn) reactions in terms of the total energy of the emitted nucleons and photons. The latter is given by the energy of the incident proton in the center-of-mass system added to the reaction Q, $E_{c.m.}+Q$, and was calculated using Wapstra's[16] mass values. It is seen that the most probable energy of the emitted neutrons and photons ranges from about 10 MeV for the (p,n) reaction to 22 MeV for the (p,4n) reaction. A similar trend is displayed in the case of the (p,pxn) reactions although the most probable energy is some 4–8 MeV larger than for the corresponding isobaric (p,xn) reaction. This difference presumably is due to the higher kinetic energy of the emitted proton.

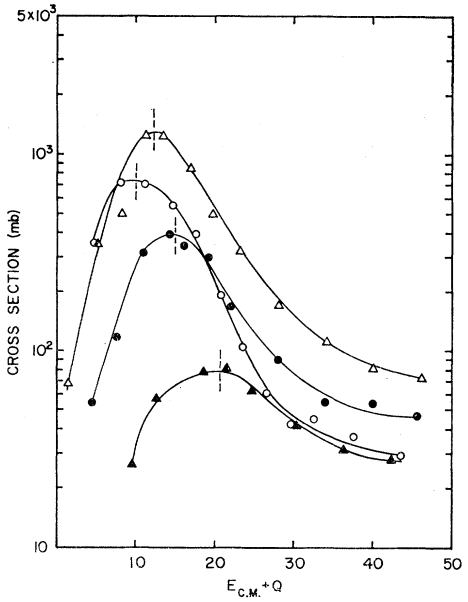

FIG. 5. Excitation functions of the (p,xn) reactions in terms of the total energy of the emitted neutrons and photons, $E_{c.m.}+Q$. ○—(p,n), △—(p,2n), •—(p,3n), ▲—(p,4n).

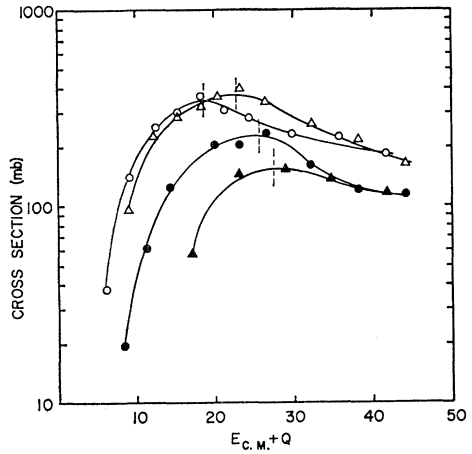

FIG. 6. Excitation functions for the (p,pxn) reactions in terms of $E_{c.m.}+Q$. ○—(p,pn); △—(p,p2n); •—(p,p3n); ▲—(p,p4n).

The experimentally determined isomer ratios (the ratios of the formation cross section of the high-spin state to that of the low-spin state) for the (p,p2n), (p,p3n), and (p,p4n) reactions are plotted in Figs. 7–9. The spins and parities of the metastable states Y^{87m}, Y^{86m}, and Y^{85m} are $(\frac{9}{2}+)$, $(8+)$ and $(\frac{1}{2}-)$, respectively, and the corresponding values of the ground states are $(\frac{1}{2}-)$, $(4-)$ and $(\frac{9}{2}+)$. It is expected that the ratios for the (p,p4n) reaction will be affected by the decay of the unknown short-lived Zr^{85} nuclide. The cascade-evaporation calculation indicates, however, that the probability of formation of Zr^{85} is only about 15–20% that of Y^{85}. Thus the contribution from Zr^{85} will affect the isomer ratios only to a small extent.

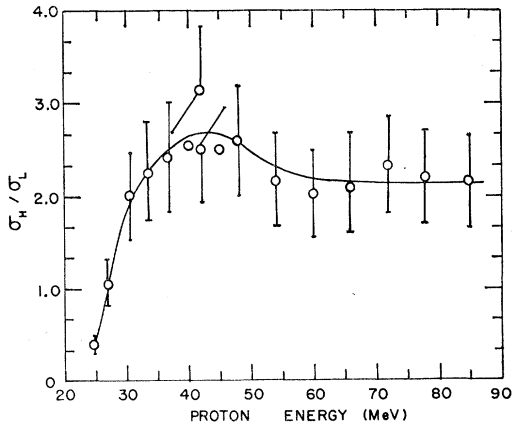

FIG. 7. Isomer ratio for the $Y^{89}(p,p2n)Y^{87m,g}$ reaction.

[16] F. Everling, L. A. König, J. H. E. Mattauch, and A. H. Wapstra, Nucl. Phys. 18, 529 (1960).

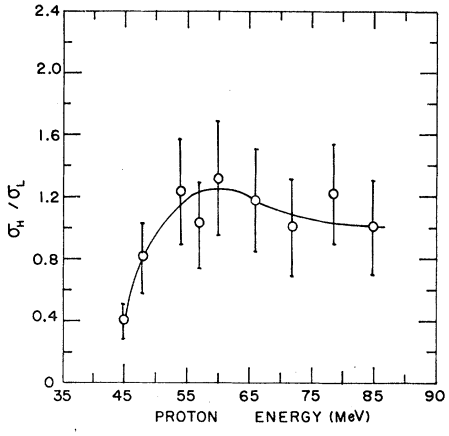

FIG. 8. Isomer ratio for the $Y^{89}(p,p3n)Y^{86m,g}$ reaction.

The isomer ratios for Y^{87} formation increase from an initial value of less than 1 at 25 MeV to a maximum of about 2.7 at 42 MeV and then decrease to a constant value of 2.2 at higher energies. Similarly, the isomer ratios for Y^{86} increase from a value of 0.4 at 45 MeV to a maximum of about 1.2 at 60 MeV and then decrease slowly at higher energies. This trend has previously been noted for similar reactions.[5,17] The initial increase is due to the fact that as the bombarding energy is increased, the orbital angular momentum brought in by the proton becomes larger, and therefore, the total angular momentum of the compound nucleus increases. Consequently, the high spin state will be increasingly favored. At higher energies direct interactions predominate resulting in a lower energy and angular momentum transfer and hence a reduction in the isomer ratio. The isomer ratios for the $(p,p4n)$ reaction have a constant value of about 2 above 65 MeV. The sharp increase noted at 60 MeV is based on a single datum and is, perhaps, not too secure.

It is to be noted that in the energy range of 45–60 MeV, the isomer ratio for the $(p,p2n)$ reaction decreases while that for the $(p,p3n)$ reaction increases. Presumably these opposing trends indicate that both compound nuclear and direct processes occur. In this energy range the excitation function for the $(p,p2n)$ reaction is already decreasing from its peak value and, as indicated before, a direct process is likely. The cross sections of the $(p,p3n)$ reaction are, on the other hand, still increasing, suggesting the likelihood of compound nucleus formation. A detailed calculation of the isomer ratios on the basis of the cascade-evaporation process will be presented in a forthcoming publication.[18]

B. Comparison with Monte Carlo Calculations

In order to make a quantitative comparison of our experimental results with the predictions of the statistical and cascade-evaporation theories, two Monte Carlo calculations have been performed. One calculation has been made according to the statistical theory assuming compound-nucleus formation throughout the energy range, i.e., up to 85 MeV, and the other according to the cascade-evaporation theory.

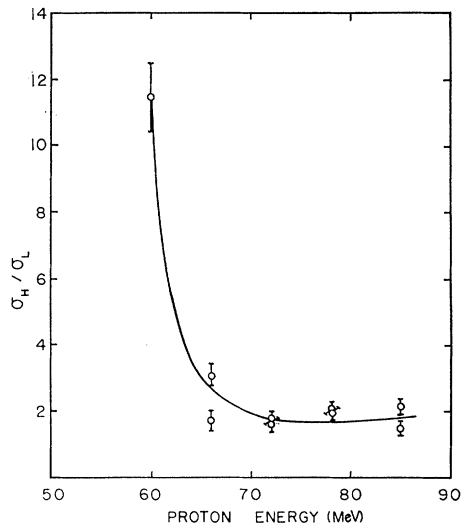

FIG. 9. Isomer ratio for the $Y^{89}(p,p4n)Y^{85m,g}$ reaction.

The recent Monte Carlo cascade calculation of Chen *et al.*[4] has been adopted for the present purpose. In this calculation the nucleus is divided into seven concentric zones of constant density and an appropriate step-function is used for the nuclear potential. Reflection and refraction of the cascade particles at the surfaces of changing potential are also considered. Five hundred cascades were run for an Y^{89} target nucleus at each of

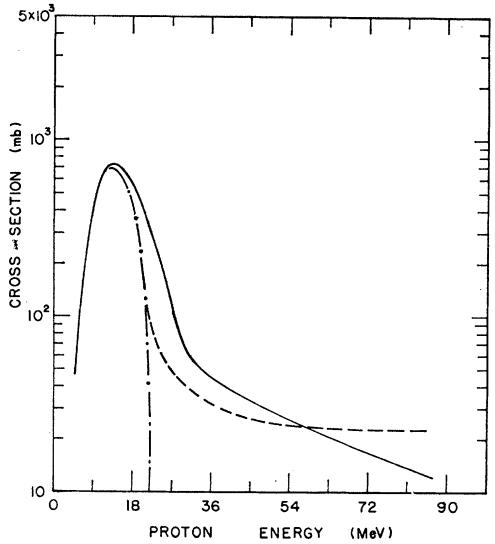

FIG. 10. Comparison of the (p,n) excitation function with statistical theory and cascade-evaporation calculations. —— experimental; —·—·—·—statistical theory; – – – cascade-evaporation.

[17] J. W. Meadows, R. M. Diamond, and R. A. Sharp, Phys. Rev. **102**, 190 (1956).
[18] G. B. Saha and N. T. Porile (to be published).

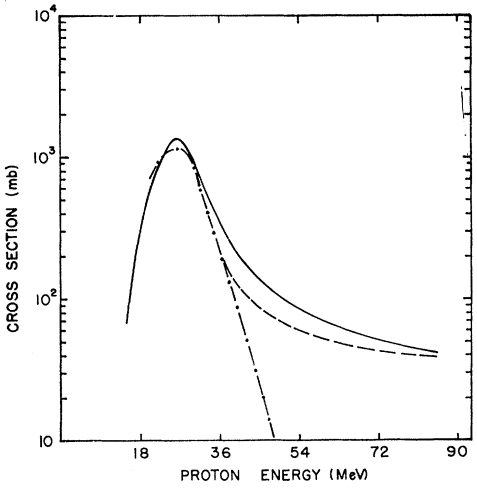

FIG. 11. Comparison of the $(p,2n)$ excitation function with theory. See Fig. 10 for details.

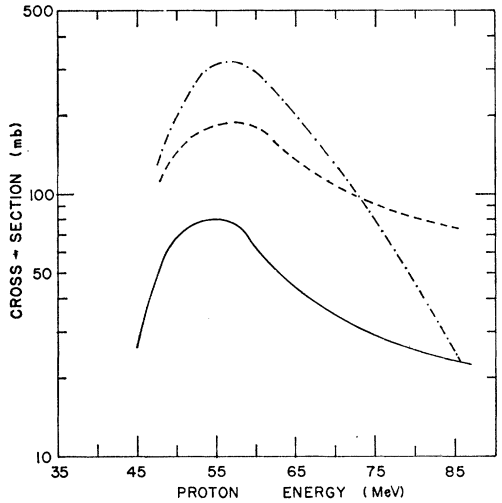

FIG. 13. Comparison of the $(p,4n)$ excitation function with theory. See Fig. 10 for details.

several incident proton energies. The residual nuclei obtained from this calculation were then used as the starting nuclei for an evaporation calculation. In order to improve the statistical accuracy of the results, three evaporation iterations were performed for each residual nucleus.

The evaporation calculation was performed on an IBM 7094 computer with a code based on the Monte Carlo treatment of Dostrovsky *et al.*[1] The inverse-reaction-cross-section constants were taken from their work for $r_0=1.5$ f. The level-density parameter was set equal to $A/20$, the mass values were taken from Wapstra,[16] and the pairing energies from Cameron.[19] The same code was used for both the evaporation part of the cascade-evaporation treatment and for the compound-nuclear calculation. The starting nucleus in the case of the latter was the Zr^{90} compound nucleus with excitation energies corresponding to several bombarding energies. One thousand evaporations were performed for each bombarding energy.

The calculated and experimental excitation functions are compared in Figs. 10–18. The following comments may be made about this comparison. First, the peak cross sections of the (p,n), $(p,2n)$, (p,pn), and $(p,p2n)$ reactions are very well reproduced by both types of calculations. The agreement between the two theories is simply a manifestation of the fact that the cascade calculation predicts nearly 100% compound nucleus formation up to 35 MeV. The remarkably good agreement between theory and experiment is probably some-

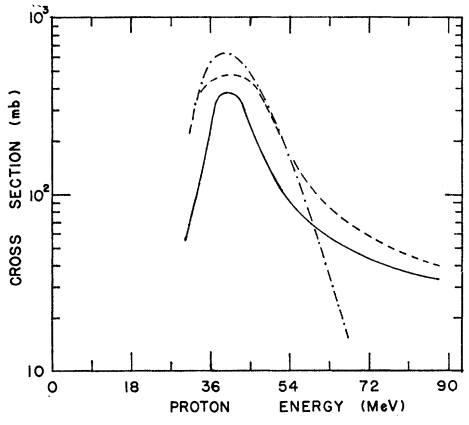

FIG. 12. Comparison of the $(p,3n)$ excitation function with theory. See Fig. 10 for details.

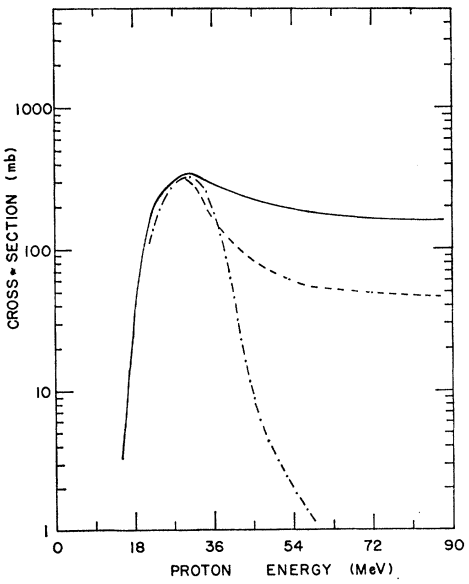

FIG. 14. Comparison of the (p,pn) excitation function with theory. See Fig. 10 for details.

[19] A. G. W. Cameron, Can. J. Phys. 36, 1040 (1958).

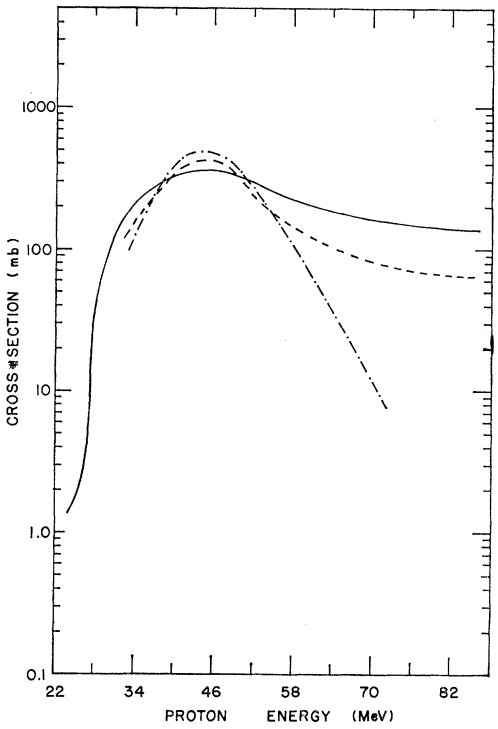

FIG. 15. Comparison of the $(p,p2n)$ excitation function with theory. See Fig. 10 for details.

what fortuitous. Previous comparisons with the Dostrovsky evaporation code[1,5] indicate that the expected agreement is only to within about 30%.

Second, the peak cross sections of the $(p,3n)$, $(p,4n)$, $(p,p3n)$, and $(p,p4n)$ reactions are grossly overestimated by the evaporation calculation. The reason for this discrepancy is the increasingly important contribution of direct processes to the simple reactions at the relatively

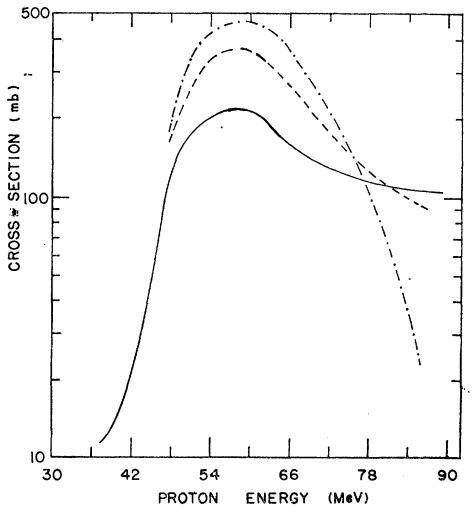

FIG. 16. Comparison of the $(p,p3n)$ excitation function with theory. See Fig. 10 for details.

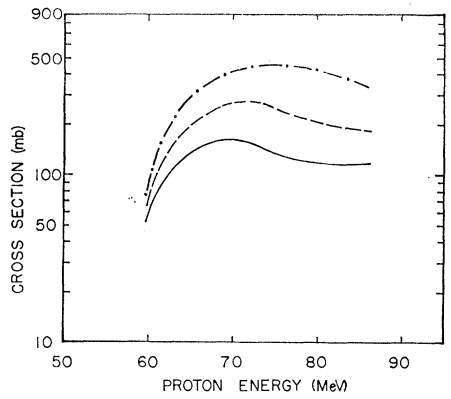

FIG. 17. Comparison of the $(p,p4n)$ excitation function with theory. See Fig. 10 for details.

high energies at which the excitation functions of these more complicated reactions peak. As a result, the cross section for compound nucleus formation becomes substantially smaller than the total reaction cross section. Since the evaporation calculation equates these two cross sections it necessarily overestimates the experimental values. This discrepancy, then, does not necessarily imply that these more complex reactions do not proceed through compound nucleus formation at the peaks of their excitation functions.

The cascade-evaporation calculation also overestimates the peak cross sections of the more complex reactions, although the discrepancy is less marked than in the case of the evaporation treatment. The reason for this result is the same as that outlined above. The

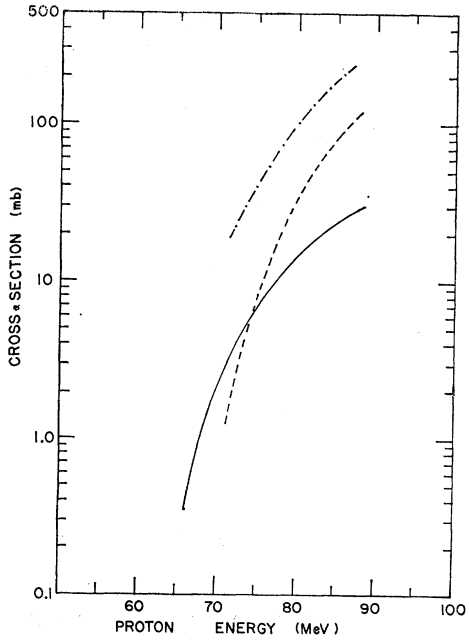

FIG. 18. Comparison of the $(p,p5n)$ excitation function with theory. See Fig. 10 for details.

cascade code thus predicts that compound nucleus formation still occurs in about 80% of the events at 50 MeV and 50% of those at 80 MeV. Evidently, these values are too large. It is of interest in this connection to note that in the same mass region, the cascade calculation of Metropolis *et al.*[2] predicted less than 50% compound nucleus formation at 50 MeV. This prediction was found to be in fairly good agreement with the cross-section measurements of Porile *et al.* on gallium.[5] It thus appears that the refinements introduced by Chen *et al.*[4] in their treatment of the knock-on cascade result in a poorer fit to low-energy data than that of the Metropolis code. This shortcoming of the calculation by Chen *et al.* may be due to an overestimate of internal reflection of the cascade particles.

Third, the evaporation calculation matches the decrease of the (p,n) and ($p,2n$) cross sections for the first 10 MeV past the peak energy. Thereafter, the statistical theory predicts cross sections that are too small by orders of magnitude. On the other hand, the cascade-evaporation calculation is in reasonable agreement with experiment throughout the entire energy range.

Fourth, the compound nuclear cross sections for the (p,pn) and ($p,p2n$) reactions become much smaller than the experimental values immediately past the peaks in the excitation functions. The cascade-evaporation cross sections are also considerably smaller than the measured values. For instance, the cross section of the (p,pn) reaction is underestimated by a factor of about 3 at 85 MeV. Evidently, the overestimation of the compound-nucleus-formation cross section at high energies is balanced by an underestimation of the cross sections of the simple (p,pxn) reactions.

The above analysis constitutes a fairly detailed test of the cascade calculation by Chen *et al.*[4] for a medium-weight nucleus at bombarding energies below 100 MeV. The validity of the evaporation code in predicting the deexcitation of the residual nuclei is attested to by the excellent agreement of the peak cross sections of the simplest reactions. The discrepancies between experiment and calculation can therefore in the main be safely attributed to the cascade code.

Our principal conclusion is that the cascade calculation overestimates the probability of compound nucleus formation above 35–40 MeV. This overestimation is primarily at the expense of the (p,pn) and ($p,p2n$) reaction cross sections. Below 35 MeV the cascade calculation correctly predicts essentially 100% compound-nucleus formation.

ACKNOWLEDGMENTS

We wish to thank Professor R. E. Bell for the use of the McGill synchrocyclotron. Dr. G. Friedlander kindly made available to us the results of the Monte Carlo cascade calculations. One of us (G.B.S.) wishes to acknowledge financial support from the National Research Council (Canada).